Computers in Biology and Medicine ▮ (▮▮▮▮) ▮▮▮–▮▮▮

Contents lists available at ScienceDirect

Computers in Biology and Medicine

journal homepage: www.elsevier.com/locate/cbm

# Probing brain connectivity by combined analysis of diffusion MRI tractography and electrocorticography

Kathrin Tertel [a,b], Nitin Tandon [a], Timothy M. Ellmore [a,*]

[a] The Vivian L. Smith Department of Neurosurgery, The University of Texas Medical School at Houston, 6431 Fannin St., MSB Suite G550F, Houston, TX 77030, USA
[b] Department of Psychology, Philipps-Universität, Marburg, Germany

ARTICLE INFO

*Article history:*
Received 22 August 2010
Accepted 11 November 2010

*Keywords:*
Electrocorticography
Diffusion-weighted MRI
Tractography
Working memory
Delay activity
Inferior fronto-occipital fasciculus
Epilepsy

ABSTRACT

Electrocorticography (ECoG) allows for measurement of task-related local field potentials directly from cortex in neurosurgical patients. Diffusion tensor imaging (DTI) tractography is an MRI technique that allows for reconstruction of brain white matter tracts, which can be used to infer structural connectivity. This paper reports a novel merger of these two modalities. A processing stream is described in which fiber tracts near intracranial macroelectrodes showing task-related functional responses are isolated to explore structural networks related to working memory maintenance. Results show that ECoG-constrained tractography is useful for revealing structural connectivity patterns related to spatially- and temporally-specific functional responses.



## 1. Introduction

Reports of novel brain structure–function relationships are increasing as neuroimaging methods are developed that relate patterns of brain white matter connectivity to cognitive processes [1–4]. At the same time, a growing number of neuroscientists are collaborating with neurologists and neurosurgeons to take advantage of the unique ability to record from subdural electrodes implanted in patients being evaluated for surgical treatment of their epilepsy [5,6]. The techniques for analyzing these two different types of data have been evolving rapidly, but separately, and there have been no systematic studies attempting to interrogate DTI tractography patterns in the context of human intracranial EEG data. A search of all journals in PubMed with the terms (ECoG and tractography) OR (electrocorticography and diffusion MRI) confirmed no published articles of studies that combine these two modalities.

In this article, a method is described showing how data from these two modalities collected in the same patient can be viewed within a common coordinate framework. This method allows DTI-based structural connectivity information to be interpreted in the context of functional information from electrocorticography (ECoG) data, which has both high spatial and temporal resolution. This method is applied to data collected during the performance of a working memory task by epilepsy patients with subdural macroelectrodes implanted in frontal, temporal, parietal and occipital lobes. Application of the method demonstrates how combining these two types of data can reveal structure–function relationships within an individual subject, and how the results may be expressed in a standard space for inter-subject comparisons.

The development of diffusion tensor imaging [7], and more recently diffusion spectrum imaging [8–10], has revolutionized the study of structural brain connectivity by allowing white matter to be reconstructed *in vivo* using safe, repeatable, and widely available MRI scanning technology. The application of deterministic and probabilistic tractography methods allows for the spatial topography of the white matter, which represents bundles coherently organized and myelinated axons [11], to be reconstructed at a resolution of 1–3 mm, depending on the specific pulse sequence used. The output of tractography algorithms may be used to answer questions about healthy and diseased structural brain connectivity. A common approach involves identifying selected known commissural, projection, or association tracts and describing their diffusion properties (i.e., integrating fractional anisotropy, or other summary tensor metrics), or identifying subcortical structures based on anatomical boundaries and asking what is the probability of a tract connecting to a particular cortical area [12]. A far smaller, but growing body of literature employs DTI tractography methods to answer questions about how functionally active brain areas are connected to each other [13–15].

The motivation for the present paper is to take advantage of several unique characteristics afforded by high-density intracranial EEG – including high spatial and temporal specificity, high signal-to-noise ratios requiring few trial presentations, minimal artifacts from subject movement, etc. – to develop a method of selecting tractography pathways based on anatomically localized functional responses. This

* Corresponding author. Tel.: +1 713 500 5443; fax: +1 713 500 0723.
*E-mail address:* Timothy.Ellmore@uth.tmc.edu (T.M. Ellmore).

0010-4825/$ - see front matter © 2010 Elsevier Ltd. All rights reserved.
doi:10.1016/j.compbiomed.2010.11.004

method is ideally suited for exploring the structural connectivity patterns of networks based on functional properties. Rather than dissecting individual fiber tracts based on anatomical landmarks, and then asking where function is located in relation to tract terminations, the present method allows one to work in the other direction: functionally interesting responses are identified, and then tracts that terminate in adjacent regions are isolated. Fiber tracts identified this way may be checked by referencing probabilistic atlases of white matter [16–18] or other standard atlases to determine their identity, or they may be candidates for novel tracts that have not been previously described, or they may include a combination of both.

The spatial proximity of tract terminations to an identified functional response is only one piece of evidence that there may be a function–structure relationship. However, it does not prove that the functional response is in any way related to an underlying connectivity pattern. To make such a conclusion, further experiments and analyses are required, both of which are addressed in the Discussion. The main objective of this paper is to outline the steps necessary to fuse the tractography and ECoG data, and to visualize the output using freely available tools.

## 2. Methodology

Imaging and ECoG data from a single epilepsy patient were used to develop the analysis methodology described in this paper. Informed written consent was obtained as part of an IRB-approved study of structural and functional characteristics of eloquent brain areas. Details of the individual imaging and electrophysiological methods are provided below, followed by a flowchart and a summary of the processing stream.

### 2.1. Image acquisition

A single pre-surgical MRI session was conducted using a 3T Philips Intera scanner (Philips Medical Systems, Bothell WA) equipped with a 16-channel SENSE head coil. First, a single high-resolution 3D T1-weighted magnetization-prepared rapid acquisition turbo field sequence (TR/TE=8.4/3.9 ms; FA=8°; matrix size=256 × 256; FOV=240 mm; slice thickness=1.0 mm thick sagittal slices) was collected, followed by a set of diffusion-weighted image volumes (32-directions, high angular resolution) using the gradient overplus option with one B0 (non-diffusion-weighted) image volume acquired before the acquisition of one repetition of the diffusion-weighted scans (TR/TE=8500/67 ms; FA=90°; matrix size 128 × 128; FOV=224 mm; 2 mm thick axial slices, max. *b*-value of 800 s/mm$^2$). Following electrode implant, a thin slice high-resolution computed tomography (CT) volume was acquired (512 × 512 matrix size, 0.5 mm in-plane resolution, 1 mm thick axial slices).

### 2.2. Image processing

MRI and CT image processing, including spatial alignment, computation of an affine normalization matrix from native subject space to a standard template (Montreal Neurological Institute N27 brain), tensor computation, and image math, was performed in AFNI [19], which is freely available online (http://afni.nimh.nih.gov/afni/download). Cortical surface reconstruction was performed using FreeSurfer (v4.5), which is extensively documented [20,21] and also freely available online (http://surfer.mnr.mgh.harvard.edu/). Surface reconstructions were visualized using the SUMA module of AFNI [22].

### 2.3. Tractography generation

After individual diffusion-weighted (DW) images volumes were realigned to the subject's skull-stripped T1 MRI, a single-model diffusion tensor was computed in AFNI with a gradient table created with the *DTI_gradient_table_creator* software written by J.A.D. Farrell (John's Hopkins University, Baltimore, MD) with each *x*, *y*, *z* gradient direction corrected by the 3 rotational alignment parameters [23]. The native-space resolution of the output realigned diffusion-weighted volumes (1.75 × 1.75 × 2.00 mm$^3$) was preserved (i.e., individual DW volumes were *not* Talairach transformed) for the purposes of computing the set of whole-brain tractography pathways. Deterministic fiber tracking was then performed using the computed native-space tensor in DTIQuery v1.1 [24] with its streamline tracking algorithm (STT) and optimal parameters [25], which included path step size=1.0 mm, seed point spacing=2.0 mm, fractional anisotropy termination threshold=0.15, angular termination threshold=45°, maximum pathway length=300 mm, and Euler's method for STT numerical integration. A set of whole-brain pathways was saved in a pathway database for further interrogation based on functional ECoG responses.

### 2.4. Working memory task

A Sternberg working memory task that has been used previously in human ECoG studies of working memory [26] was used for the ECoG working memory recordings. In this task, serially presented random letters are displayed, followed by a delay period, and then by a yes/no decision made by button press to signal whether a single probe letter was seen before the delay. Fifty trials of this task were completed per session with the patient viewing the task on an LCD monitor while seated comfortably in a bed in the hospital's epilepsy monitoring unit.

### 2.5. ECoG acquisition

ECoG data were sampled at 1 kHz using an EEG 1100 Nihon Koden Neurofax clinical acquisition system. The number and placement of the grids and strips of macroelectrodes were determined by clinical considerations. For each memory task trial, event times for the onset and offset of each item presentation, the start and end of the delay interval, and the onset and offset of each probe stimulus were sent to an isolated continuously sampled recording channel by a TTL pulse in order to synchronize the task trial onsets with ECoG data. All data were digitally re-referenced to a common average reference taken from all channels excluding those channels with noise (i.e., 60 Hz artifacts), any electrodes with ictal activity, and any electrodes adjacent to brain tissue that was eventually resected to treat the epilepsy.

### 2.6. ECoG processing

To assess delay period activity, defined as a sustained functional response related to memory maintenance, signal processing at each electrode channel involved analytical decomposition and computation of time–frequency power spectra (Fig. 2) as described in [27,28] and implemented in Matlab (R2010a, Mathworks, Natick MA). This process is analogous to a Gabor wavelet analysis in the temporal domain, but is performed in the frequency domain for speed. Briefly, each signal was Fourier-transformed from the time to frequency domain, multiplied by the overlapping Gaussians centered at multiple frequencies of interest (50 frequencies, min. freq=1.0 Hz, max. freq=200 Hz, fractional bandwidth=0.2), and then inverse Fourier-transformed back to the time domain. The resulting analytic signal had an equal number of time points as the original raw signal, but contained a number of orthogonal representations equal to the 50 different frequencies of interest. Power was calculated from the amplitude of analytic signal, and used to

Please cite this article as: K. Tertel, et al., Probing brain connectivity by combined analysis of diffusion MRI tractography and electrocorticography, Comput. Biol. Med. (2010), doi:10.1016/j.compbiomed.2010.11.004

build time–frequency power spectra for two different epochs of the task, the delay interval and a pre-trial baseline interval.

ECoG signals were recorded continuously during the performance of 50 trials of the working memory paradigm. For each trial, after the serial presentation of letter (i.e., item) strings, a 2 s delay period followed during which the monitor was completely blank (color black). For each channel, power spectra were computed for each of these 50 delay periods, resulting in a matrix of power spectra of size 50 (trials) $\times$ 50 (frequencies) $\times$ 2000 (time in ms) and another $50 \times 50 \times 2000$ matrix of power spectra were computed for a baseline period taken between the beginning and end of each trial. At each channel, the matrices of spectra were averaged to produce a mean power spectrum for the delay period, $P_d$, and a mean power spectrum for the baseline period, $P_b$. These mean spectra were subtracted and normalized by trial-to-trial variance with no assumption of similar variance in the delay and baseline periods using the following equation: $(P_d - P_b)/\mathrm{sqrt}((s_d^2/n_d) + (s_b^2/n_b))$, where $s$ is the variance over $n = 50$ trials. Thus, at each channel a single power spectrum of size 50 (frequency) $\times$ 2000 (time) was computed with each element representing a standardized power difference, equivalent to a $t$-statistic, between the delay and baseline periods.

### 2.7. Description of processing stream

A flowchart summarizing the computational processing steps is shown in Fig. 1, and the important steps are summarized here.

The pre-surgical T1-weighted structural MRI defines the single-subject analysis space. Consequently, the pre-surgical individual DW volumes and post-surgical CT volume with implanted electrodes are each aligned to the T1 MRI. A 12-parameter affine transformation of the T1 MRI to standard Talairach space is also performed at this stage, and the resultant $4 \times 4$ transformation matrix is stored for use later. Cortical surface and white/gray matter border reconstructions in native single-subject space are also generated from the T1 MRI. The aligned DW volumes and the set of 32 diffusion gradient directions corrected by the 3 rotational alignment parameters are used to compute a diffusion tensor [23]. From this tensor, a set of whole-brain tractography streamlines is generated. Calculations of the diffusion tensor and whole-brain tractography pathways were deliberately performed in the native image space as defined by the T1-weighted anatomical. A stored transformation of the T1 anatomical volume to standard space was applied to selected native-space tractography pathways after isolation based on nearby electrode responses. We avoided computation of the tensor and tractography pathways from Talairach-transformed diffusion image volumes as this would require an additional correction of the gradient orientations by the three $x$-, $y$-, and $z$-axis rotations required to put each diffusion image volume into Talairach space (see [23]). Furthermore, we are hesitant to compute a tensor and pathways from spatially normalized diffusion volumes because of uncertainty about how stretching of a native-space brain to a template may result in creation of new pathways or elimination/compression of existing pathways when tractography algorithms are applied to normalized data.

The electrode contacts on the aligned CT volume appear as bright (i.e., signal intensity value is higher than any biological tissue) well-defined artifacts with centers that are easily identifiable. The center coordinates are located for each electrode by

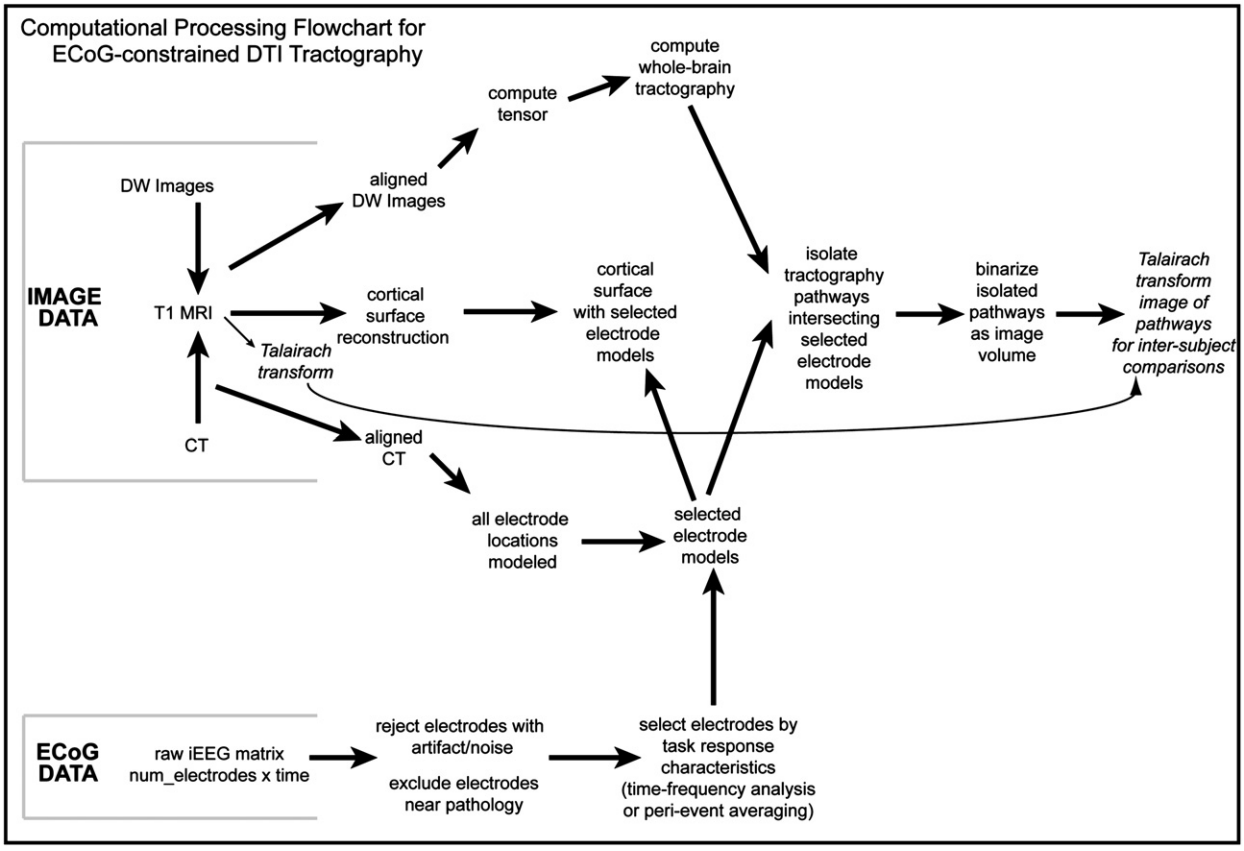


**Fig. 1.** Computational processing flowchart for ECoG-constrained tractography. Arrows indicate temporal order of processing. Image analysis, including diffusion tensor calculation and computation of each subject's whole-brain tractography pathways, is performed in the native image space defined by the T1-weighted anatomical MRI. After selected tractography pathways are isolated based on nearby electrode responses, a stored 12 parameter affine transformation of the T1 volume to Talairach space is applied to the set of pathways so that an image volume in standard space can be used for inter-subject comparisons.

Please cite this article as: K. Tertel, et al., Probing brain connectivity by combined analysis of diffusion MRI tractography and electrocorticography, Comput. Biol. Med. (2010), doi:10.1016/j.compbiomed.2010.11.004

computing a center of mass. Due to non-linear deformation of the brain caused by the implantation of grids and strips of electrodes [29], these centers often appear buried just below the cortical surface representation generated from the pre-surgical MRI. The amount of distortion can vary from patient to patient, and depend on factors like the location of the craniotomy, the number and placement of electrodes, and the presence and severity of any post-surgical swelling. The distortion relative to the cortical surface reconstruction computed from the high resolution pre-surgical T1 MRI is manifest as a medial shift of 1–4 mm (making electrodes appear to be below the pre-surgical cortical surface), and lateral shifts in the anterior–posterior or superior–inferior direction of as many as 12 mm. To correct for this, a normal line is projected from each center coordinate perpendicular to the nearest surface node. The coordinate of the nearest intersected surface node is used as the new electrode center coordinate, and this new coordinate may be further adjusted, if necessary, using intra-operative photographs of electrode locations relative to gyral/sulcal anatomy taken during the electrode implant and explant procedures. Our method for localizing electrodes relative to pre-surgical cortical geometry is conceptually similar to other approaches reported in the literature [30,31]. Furthermore, in our application, all alignments are confirmed by photographs taken at explantation (removal of electrodes) allowing for the brain shifts to be corrected and the electrode locations with respect to the cortical surface model to be confirmed in the second surgery. Once each electrode center is assigned a coordinate on the cortical surface (pial layer approximation), a spherical model is made of each electrode. While each electrode contact is a 2.5 mm diameter platinum/iridium concentric disk, a spherical model with a larger radius ($r=4.0$ mm) is generated to extend the electrode inwards to the white/gray matter border, where most tractography pathways terminate, and to extend the coverage of the model to include adjacent tissue, since signals distal to electrode contact that have been shown to contribute to the recorded local field potential [32,33]. At this stage, all electrodes are displayed on the cortical surface reconstruction using SUMA.

Processing of the ECoG data begins with inspection of each electrode's raw and time–frequency domain power spectral signature to identify channels with artifact (i.e., 60 Hz line noise). These channels are excluded from further analysis, as are electrodes overlaying areas of pathology (i.e., epileptogenic areas) and electrodes overlaying brain tissue that was resected during the explant procedure (after recording task-related ECoG) to treat the epilepsy. The remaining electrode channels are subjected to analysis of task response characteristics, including peri-event averaging (where an event is the visual stimulus onset during the encoding and retrieval phases of the memory task) and time–frequency analysis of the delay period compared to a pre-trial baseline. Electrodes of interest are selected based on their evoked response to visual stimulation, as well as sustained frequency-specific (i.e., gamma-band) responses during the delay minus baseline period. A focus on the gamma band is motivated by evidence that neural synchrony in this frequency range is increased during working memory maintenance [34–36] and during other aspects of vision, such as awareness [37].

Once a subset of electrodes is selected based on task-related response characteristics, the spherical models corresponding to these electrodes are passed as input to a function written in Matlab, which also takes as another input the set of whole-brain tractography pathways. This function checks the coordinates of each tractography pathway's terminations, and if any termination is located within the spatial vicinity of the spherical electrode model, the entire pathway is saved in a database file for further visualization and analysis. An image volume of these pathways is also created with an integer value at each voxel that represents the number of pathways passing through the imaging element. Since the saved pathways and the associated image volume shares the coordinate space of the T1 MRI, the $4\times4$ transformation to Talairach space may be applied to bring the pathway coordinates and a binarized image volume representation of these pathways into a standard space for inter-subject group comparisons.

## 3. Application

Working memory ECoG data was obtained from an epilepsy patient (male, age 26, right-handed) implanted with grids and strips of electrodes in his left hemisphere. Despite having a focal cortical resection in his left lateral temporal lobe several years before (that did not eliminate his seizures), he performed exceptionally well on the task, answering 48 of 50 trials correctly (96%) with an average reaction time of 602.24 ($\pm$117.28) ms. The patient had widespread electrode coverage with strips placed over the parieto-occipital region, and multiple grids placed over dorsolateral prefrontal cortex and the peri-sylvian areas. Combining his ECoG and DTI data presented a good test case to address a specific question about connectivity underlying visual working memory: specifically, what are the fiber pathways that convey visual information from posterior cortical areas to frontal areas and are implicated in the short term maintenance of visual information [38]? Analysis of the ECoG signals proceeded by identifying a subset of electrodes with elevated (relative to a pre-trial baseline) gamma-band power during the 2 s delay period after letter stimuli were presented.

An electrode on the left lateral $1\times4$ occipital strip overlaying middle occipital gyrus (Fig. 2a, posterior red electrode, Talairach coordinate: $x=-24$, $y=-91$, $z=22$) was found to have a large increase in gamma power during the delay interval.

No other electrodes on the occipital strip showed sustained elevated gamma power during the delay interval, although a neighboring electrode showed strong peri-event responses to the visual presentation of letters during the encoding and probe trial, but no sustained delay activity.

Based on the significant ($p<0.01$) change in gamma oscillatory power on the lone occipital electrode, it was decided to isolate the tractography pathways terminating in region immediately adjacent to the electrode's contact with cortex (Fig. 3). A large number (552) of pathways were isolated that terminated in the region around this electrode. The trajectory of these pathways was examined, and the vast majority connected to brain areas located anteriorly. One subset of these pathways consisted of the inferior fronto-occipital fasciculus (IFoF), which terminates in ventrolateral frontal lobe. The IFoF is a fiber tract that has been implicated in visual neglect [39], in verbal memory processes [4,40] (left hemisphere), and in arithmetic calculation [41] (right hemisphere). Another subset of pathways isolated near the occipital electrode consisted of the inferior longitudinal fasciulus (ILF) connecting the region around the electrode to anterior temporal lobe. Yet another component (not visible in Fig. 3) consisted of commissural pathways connecting inter-hemispheric areas of the occipital lobe.

The frontal terminations of the IFoF (green pathways Fig. 3c) were located near one of the electrodes of a fronto-polar electrode strip (Fig. 3b, red anterior electrode, Talairach coordinate: $x=-52$, $y=31$, $z=9$). This electrode also demonstrated a significant change in delay period gamma power (Fig. 2b), and it was decided to isolate the tractography pathways near this electrode to determine their relationship with the IFoF terminations. A substantial number (100) of pathways were isolated near this electrode (Fig. 3c, blue pathways). Most ran parallel to the IFoF pathways for a short distance, but connected anterior thalamus and other occipital–temporal areas. A small number (3) connected directly to the region

Please cite this article as: K. Tertel, et al., Probing brain connectivity by combined analysis of diffusion MRI tractography and electrocorticography, Comput. Biol. Med. (2010), doi:10.1016/j.compbiomed.2010.11.004

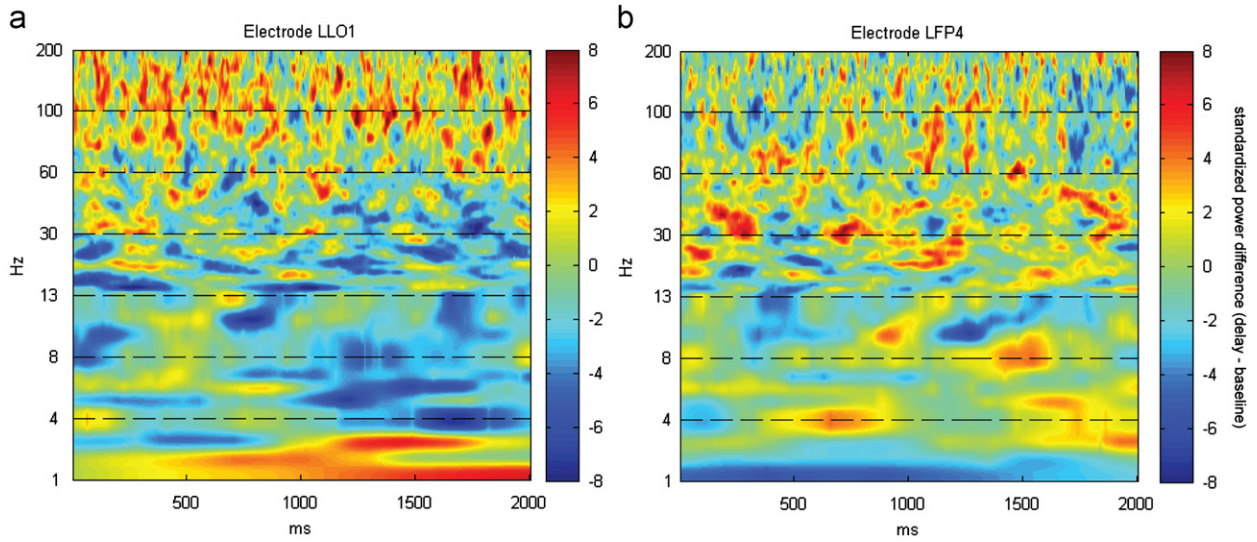


**Fig. 2.** Power spectra show sustained functional responses during the delay period. Time (*x*-axis) × frequency (*y*-axis) power spectra for (a) occipital electrode LLO1 and (b) frontal electrode LFP4. Displayed are power differences between the delay and baseline period of the working memory task, where positive difference (yellow to red) indicates higher power in the delay period than in the baseline period. All power differences are in standard deviations. (For interpretation of the references to color in this figure legend, the reader is referred to the web version of this article.)

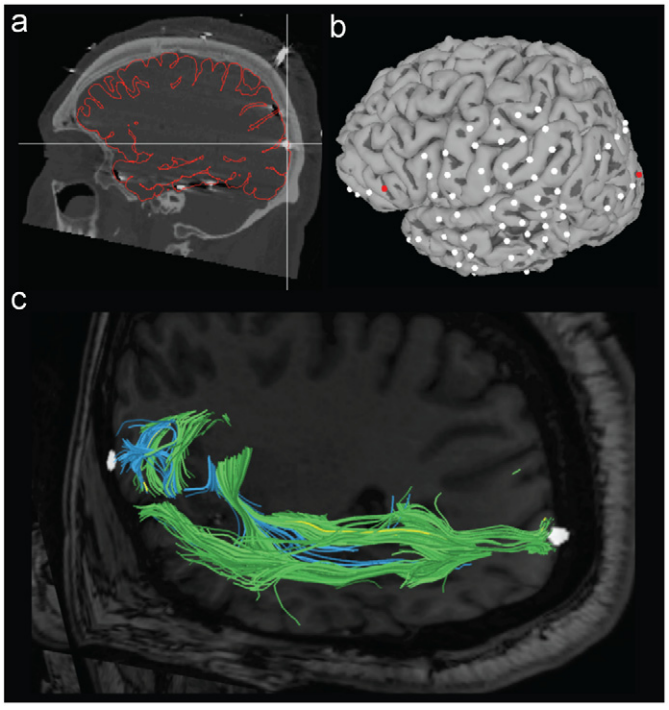


**Fig. 3.** Electrode localization and functionally-constrained MR diffusion tractography pathways in a single patient. (a) CT scan of patient with intracranial electrodes visible as bright intensity regions. Outlines of the reconstructed cortex are indicated in red, each electrode presents itself as an artifact (occipital electrode highlighted by crosshairs), (b) Surface model of the brain generated from T1-weighted MRI with electrodes, whose coordinates were found on the CT scan and then modeled on the reconstructed cortical surface. Red electrodes (frontal and occipital) showed significantly higher gamma power during working memory delay compared to baseline and (c) White matter tracts (green, blue, and yellow) adjacent to frontal and occipital gamma electrodes (white spheres). Green pathways have terminations in brain tissue adjacent to the occipital electrode, blue pathways to the area around the frontal electrode, and yellow pathways terminate near both electrodes. (For interpretation of the references to color in this figure legend, the reader is referred to the web version of this article.)

near the occipital electrode (Fig. 3c, yellow pathways). Considering that a fraction of the bundle of IFoF pathways isolated from the occipital electrode terminated near the frontal electrode, and that both electrodes showed elevated gamma power, a correlation of the time–frequency spectrograms from both electrodes was computed to determine if there was a relationship between frequency-specific power across the delay period. An *a priori* threshold of $p < 0.01$ was corrected for multiple comparisons by dividing the significance level by 2000 (number of delay period time bins) times 7 (number of frequency bands), and positive and negative correlations exceeding this corrected threshold were noted. Positive correlations were found in the low-gamma ($r=0.08$) and the mid-gamma ($r=0.12$) bands; negative correlations were found in the delta ($r=-0.24$), theta ($r=-0.06$), and beta ($r=-0.08$) bands. These inter-regional correlations in gamma-band activity are numerically low, but are typical of high temporal resolution neural data, where even intra-regional spike correlations are often low in magnitude [42]. Thus, in addition to the evidence of structural connectivity provided by tractography, there was some evidence that the brain areas near these electrodes were also *functionally* connected as demonstrated by correlated activity in the gamma band.

The single-subject analysis presented here is one example of the rich type of data exploration that may be conducted using the method of ECoG-constrained tractography. Tractography connectivity among all electrodes constrained by functional activity in any frequency band during any task component could be investigated. To confirm the specific structure–function relationship involving the IFoF reported here for a single patient, a larger sample of patients with a similar distribution of electrode coverage would be needed.

To demonstrate how the functionally-constrained pathway output presented here for one patient may be used to create group-level white matter maps, all electrodes showing significant (greater than a 2 standard deviation change from baseline) delay period gamma power increases were identified in 9 epilepsy patients. From a total of 629 noise-free electrodes overlaying non-pathological tissue, 74 (11.8%) were found that had elevated gamma power during the delay period of the working memory task. Tractography pathways terminating in the vicinity of these electrodes were isolated, binarized as image volumes, transformed to Talairach space, and summed to create maps with voxel values equal to the number of subjects with at least 1 gamma-related pathway. The summed map can be visualized in volume space or, as

Please cite this article as: K. Tertel, et al., Probing brain connectivity by combined analysis of diffusion MRI tractography and electrocorticography, Comput. Biol. Med. (2010), doi:10.1016/j.compbiomed.2010.11.004

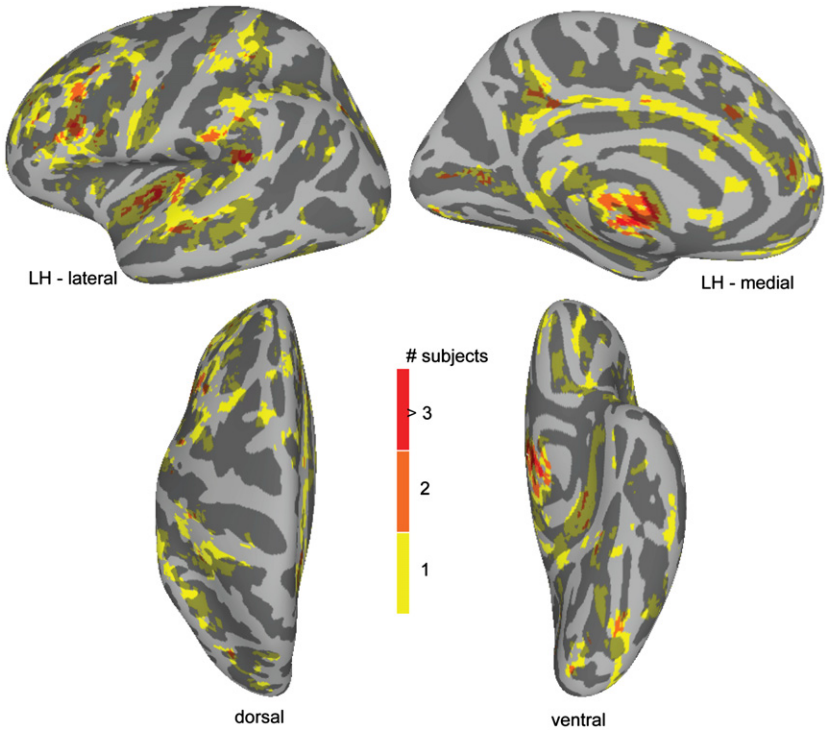


**Fig. 4.** Group analysis of tractography pathways adjacent to electrodes with delay period gamma power increases. Tractography pathway terminations are displayed on an inflated representation of a left hemisphere in Talairach space. Areas colored in yellow, red and orange represent tractography pathway terminations computed from 9 patients. The terminations are from tractography pathways located adjacent to electrodes showing a significant gamma response during a working memory delay period. Terminations unique to one patient are yellow, common to two patients are orange, and common to three or more patients are colored red. (For interpretation of the references to color in this figure legend, the reader is referred to the web version of this article.)

shown in Fig. 4, can be painted on an average standard-space inflated cortical surface reconstruction [21]. This visualization reveals several areas, where 3 or more subjects show gamma-related white matter terminations, and can be used to identify common nodes that are connected by white matter tractography pathways. It should be noted that even though data from 9 patients were used to create these summary maps, electrode coverage was not uniform across patients and many cortical areas, most notably parietal cortex, were undersampled. Therefore, while the colored areas in Fig. 4 represent terminations of white matter pathways related to delay period gamma oscillations, the absence of color does not imply that these areas do not also contain important terminations. Additional subjects with electrodes covering the undersampled areas would have to be included to make firmer statements about whole-brain network connectivity.

## 4. Discussion

In this paper a means of interrogating diffusion MRI tractography data by way of functional information obtained using intracranial EEG data is described. Isolating fiber tracts based on nearby functional responses represents one of many ways that diffusion tractography data may be queried to investigate patterns of connectivity. Other modalities may be used to select tracts based on function. It is entirely feasible to use fMRI-BOLD activation patterns that are statistically significant either within or between subjects to constrain pathway selection. While spatially precise (fMRI voxels sizes typically range from 1 to 4 mm), the functional BOLD response is temporally lagged due to hemodynamics and therefore does not have the millisecond resolution of ECoG. Constraining tract selection based on event-related or time–frequency magnetoencephalography (MEG) responses is also possible. While MEG has high temporal resolution, it suffers from some degree of spatial uncertainty about precisely where the electromagnetic response originates, although information about the geometry of the cortical surface can improve source localization [43]. The main advantage of ECoG-constrained tractography is that it has both high temporal (ms) and spatial (mm) resolution. And since the electrodes are placed below the dura directly on cortex, far fewer trials are required when averaging to obtain significant responses.

In the examples described in this paper, whole-brain tractography pathways were analyzed in relationship to electrode locations showing sustained gamma-band power increases during a visual letter working memory delay period. The network connectivity underlying working memory is a topic of great interest in neuroscience, and the task employed in the present study has already been described and validated by others. Therefore it was an ideal test case for developing the method, but in practice any cognitive task or even resting rhythms during wakefulness or sleep could be used to probe structural connectivity. One promising future application is to discover in humans the generators and networks underlying frequency-specific rhythms. For example, what are the networks underlying the human theta rhythm, or which brain networks are implicated in the reported phase-locking of the high gamma rhythm to the theta rhythm [44]? Application of ECoG constrained tractography to answer questions about the genesis of brain oscillations is promising, but a major limiting factor is that only some brain areas are covered by electrodes and this is dictated solely by clinical criteria. To make conclusive statements about how white matter networks are related to brain oscillations will require a large sample of patients implanted with large numbers of electrodes in cortical and subcortical areas. While many epilepsy patients are implanted with cortical electrodes, fewer receive electrode implants in deep brain structures like the

Please cite this article as: K. Tertel, et al., Probing brain connectivity by combined analysis of diffusion MRI tractography and electrocorticography, Comput. Biol. Med. (2010), doi:10.1016/j.compbiomed.2010.11.004

amygdala and hippocampus. Other structures like the thalamus are rarely but sometimes implanted with electrodes [45], but one could in theory examine white matter related to electrical recordings taken from these and other areas, like the basal ganglia and subthalamic nucleus in Parkinson's patients and the subgenual cingulate gyrus in severe depression patients undergoing treatment with deep brain stimulation [46,47]. Another promising application is to apply the method to uncover tracts connecting neocortical areas that demonstrate gamma LFP-BOLD coupling [48], and to explore the degree of overlap with networks related to hippocampal theta LFP-BOLD coupling [49].

Implantation of macroelectrodes in epilepsy patients brings with it the added advantage of being able to deliver electrical stimulation through the electrode contacts, which is frequently done for clinical identification of eloquent cortex but often yields unexpected and interesting research findings [50]. Stimulation of electrode contacts is also helpful for answering questions about functional connectivity [51]. For example, if task-related responses are found on two distant electrodes, and then ECoG-constrained tractography is used to show that tractography pathways exist between the two electrode locations, then electrical stimulation through each contact can be carried out to elicit cortico-cortical evoked potentials, the magnitude and latency of which can be measured to obtain further evidence that the brain areas being recorded from by these electrodes are functionally connected. In the absence of stimulation, a correlation of the ECoG timecourses between the distant electrodes during a rest period may also be taken as evidence of functional connectivity.

ECoG-constrained tractography is certainly not without limitations, some of which are major. The main limitation is that intracranial EEG in humans can only be obtained in neurosurgical patients, most commonly patients with pharmaco-resistant epilepsy. Electrode locations must be carefully examined with respect to the each patient's clinical EEG and surgical resection plan to avoid areas of known pathology, and task-related functional responses and the channels across the entire recording session must be inspected for ictal activity. Even when responses are considered from only electrodes overlaying healthy brain tissue, the underlying brain connectivity patterns may have been shaped by years of epileptic activity. Since so little is known about the relationship between pathology of epileptogenic cortex and diffusion imaging patterns, converging evidence is needed to confirm that novel pathways identified using ECoG-constrained tractography actually exist in healthy control subjects. Since ECoG is not obtainable in healthy controls, alternative methods like fMRI, MEG, or even near infrared spectroscopy (NIRS), could be used to corroborate the existence of task-related responses near the termination zones of identified tracts.

Another limitation of ECoG-constrained tractography relates to an assumption about anatomical connectivity. If a brain region shows a task-related functional response, but no long-range (i.e., inter-lobar), commissural (i.e., inter-hemispheric) or projection (cortico-subcortical) pathways are found in the immediate region where the electrode makes contact with cortex, one cannot conclude that this area is not a structural node of a task-related functional network. That is because there may be short-range, cortico-cortical pathways that connect this region with, for example, a neighboring gyrus where long-range pathways in turn project to another eloquent region. Cortico-cortical pathways are likely important components of brain networks. Empirical support for the functional relevance of these short pathways comes from a diffusion MR tractography study of the language system in which a large number of intraoperative cortical stimulation sites were shown to be located near cortico-cortical pathways that terminate in the same brain regions as terminations of pathways comprising the arcuate fasciculus [52]. The incorporation of short cortico-cortical pathways into network maps isolated from functional responses is possible; it can be done using the deterministic tractography methods employed in the present study by including a pathway length range as an additional spatial inclusion criterion. Cortico-cortical pathways are also likely to be included in functionally-defined structural connectivity networks when probabilistic algorithms are substituted for the deterministic methods in the processing framework outlined here, which is feasible if the spherical electrode models are simply treated as seed region inputs to the probabilistic tracking algorithm.

## 5. Summary

A method for constraining whole-brain tractrography using functional responses from electrocorticography in epilepsy patients implanted with large numbers of subdural macroelectrodes is described. The novel merger of these two types of data allows exploration of connectivity patterns using human neural recordings with high spatial and temporal precision. The computational method used to fuse these data representations is advantageous based on its modularity, utilization of freely-available imaging tools, and easy manipulation of critical parameters, such as the model of space sampled by the electrode and the ability to substitute the type of tractography algorithm employed on the processed diffusion-weighted images. Application of the method is demonstrated by example analysis of a single patient dataset where pathways of the IFoF, a tract recently implicated in visual and memory processes, were isolated based on ECoG time–frequency delay period gamma-band responses. An example is also provided to show how the method may be used to make population inferences based on binarized white matter representations transformed to standard space. The isolation of structural connectivity patterns near electrodes showing similar functional responses does not necessarily mean the brain regions near the electrodes are necessary for neural computation, but this method provides the framework for further investigation of function–structure relationships using additional experimental manipulations like direct electrical stimulation and resting-state coherence analysis.

## Conflict of interest statement

None declared.

## Acknowledgements

We thank Vipulkumar S. Patel for help in collecting the MRI data, and Faraz Khursheed, Michael DiSano, and Tom Pieters for help with data collection and analysis. K.T. was awarded funding from The University of Texas Graduate School of Biomedical Sciences to complete this work as part of a summer research internship. N.T. is supported by a K12 career development award from NIH. T.M.E. is supported by a research grant from the Epilepsy Foundation. Support was also provided by R01DA026452 and The Vivian L. Smith Foundation for Neurological Research.

## References

[1] T.M. Ellmore, M.S. Beauchamp, J.I. Breier, J.D. Slater, G.P. Kalamangalam, T.J. O'Neill, et al., Temporal lobe white matter asymmetry and language laterality in epilepsy patients, NeuroImage 49 (3) (2010) 2033–2044.

[2] S.R. Rudebeck, J. Scholz, R. Millington, G. Rohenkohl, H. Johansen-Berg, A.C. Lee, Fornix microstructure correlates with recollection but not familiarity memory, Journal of Neuroscience 29 (47) (2009) 14987–14992.

[3] M. Catani, M.P. Allin, M. Husain, L. Pugliese, M.M. Mesulam, R.M. Murray, et al., Symmetries in human brain language pathways correlate with verbal recall,

Proceedings of the National Academy of Sciences of the United States of America 104 (43) (2007) 17163–17168.
[4] C.R. McDonald, M.E. Ahmadi, D.J. Hagler, E.S. Tecoma, V.J. Iragui, L. Gharapetian, et al., Diffusion tensor imaging correlates of memory and language impairments in temporal lobe epilepsy, Neurology 71 (23) (2008) 1869–1876.
[5] N.E. Crone, A. Sinai, A. Korzeniewska, High-frequency gamma oscillations and human brain mapping with electrocorticography, Progress in Brain Research 159 (2006) 275–295.
[6] K. Jerbi, T. Ossandon, C.M. Hamame, S. Senova, S.S. Dalal, J. Jung, et al., Task-related gamma-band dynamics from an intracerebral perspective: review and implications for surface EEG and MEG, Human Brain Mapping 30 (6) (2009) 1758–1771.
[7] P.J. Basser, Inferring microstructural features and the physiological state of tissues from diffusion-weighted images, NMR in Biomedicine 8 (7–8) (1995) 333–344.
[8] D.S. Tuch, T.G. Reese, M.R. Wiegell, V.J. Wedeen, Diffusion MRI of complex neural architecture, Neuron 40 (5) (2003) 885–895.
[9] V.J. Wedeen, P. Hagmann, W.Y. Tseng, T.G. Reese, R.M. Weisskoff, Mapping complex tissue architecture with diffusion spectrum magnetic resonance imaging, Magnetic Resonance in Medicine 54 (6) (2005) 1377–1386.
[10] V.J. Wedeen, R.P. Wang, J.D. Schmahmann, T. Benner, W.Y. Tseng, G. Dai, et al., Diffusion spectrum magnetic resonance imaging (DSI) tractography of crossing fibers, NeuroImage 41 (4) (2008) 1267–1277.
[11] S.K. Song, S.W. Sun, M.J. Ramsbottom, C. Chang, J. Russell, A.H. Cross, Dysmyelination revealed through MRI as increased radial (but unchanged axial) diffusion of water, NeuroImage 17 (3) (2002) 1429–1436.
[12] T.E. Behrens, H. Johansen-Berg, M.W. Woolrich, S.M. Smith, C.A. Wheeler-Kingshott, P.A. Boulby, et al., Non-invasive mapping of connections between human thalamus and cortex using diffusion imaging, Nature Neuroscience 6 (7) (2003) 750–757.
[13] R. Kleiser, P. Staempfli, A. Valavanis, P. Boesiger, S. Kollias, Impact of fMRI-guided advanced DTI fiber tracking techniques on their clinical applications in patients with brain tumors, Neuroradiology 52 (1) (2010) 37–46.
[14] J.C. Wilcke, R.P. O'Shea, R. Watts, Frontoparietal activity and its structural connectivity in binocular rivalry, Brain Research 11 (2009) 96–107.
[15] P. Staempfli, C. Reischauer, T. Jaermann, A. Valavanis, S. Kollias, P. Boesiger, Combining fMRI and DTI: a framework for exploring the limits of fMRI-guided DTI fiber tracking and for verifying DTI-based fiber tractography results, NeuroImage 39 (1) (2008) 119–126.
[16] K. Hua, J. Zhang, S. Wakana, H. Jiang, X. Li, D.S. Reich, et al., Tract probability maps in stereotaxic spaces: analyses of white matter anatomy and tract-specific quantification, NeuroImage 39 (1) (2008) 336–347.
[17] Y. Zhang, J. Zhang, K. Oishi, A.V. Faria, H. Jiang, X. Li, et al., Atlas-guided tract reconstruction for automated and comprehensive examination of the white matter anatomy, NeuroImage (2010).
[18] D.J. Hagler Jr., M.E. Ahmadi, J. Kuperman, D. Holland, C.R. McDonald, E. Halgren, et al., Automated white-matter tractography using a probabilistic diffusion tensor atlas: application to temporal lobe epilepsy, Human Brain Mapping 30 (5) (2009) 1535–1547.
[19] R.W. Cox, AFNI: software for analysis and visualization of functional magnetic resonance neuroimages, Computers and Biomedical Research, An International Journal 29 (3) (1996) 162–173.
[20] A.M. Dale, B. Fischl, M.I. Sereno, Cortical surface-based analysis. I. segmentation and surface reconstruction, NeuroImage 9 (2) (1999) 179–194.
[21] B. Fischl, M.I. Sereno, A.M. Dale, Cortical surface-based analysis. II: inflation, flattening, and a surface-based coordinate system, NeuroImage 9 (2) (1999) 195–207.
[22] Z.S. Saad, R.C. Reynolds, B. Argall, S. Japee, R.W. Cox, SUMA: An Interface for Surface-Based Intra- and Inter-Subject Analysis with AFNI, Proceedings of the Second IEEE International Symposium on Biomedical Imaging: Macro to Nano 2 (2004) 1510–1513.
[23] A. Leemans, D.K. Jones, The B-matrix must be rotated when correcting for subject motion in DTI data, Magnetic Resonance in Medicine 61 (6) (2009) 1336–1349.
[24] A. Sherbondy, D. Akers, R. Mackenzie, R. Dougherty, B. Wandell, Exploring connectivity of the brain's white matter with dynamic queries, IEEE Transactions on Visualization and Computer Graphics 11 (4) (2005) 419–430.
[25] P.J. Basser, S. Pajevic, C. Pierpaoli, J. Duda, A. Aldroubi, In vivo fiber tractography using DT-MRI data, Magnetic Resonance in Medicine 44 (4) (2000) 625–632.
[26] S. Raghavachari, M.J. Kahana, D.S. Rizzuto, J.B. Caplan, M.P. Kirschen, B. Bourgeois, et al., Gating of human theta oscillations by a working memory task, Journal of Neuroscience 21 (9) (2001) 3175–3183.
[27] R.T. Canolty, M. Soltani, S.S. Dalal, E. Edwards, N.F. Dronkers, S.S. Nagarajan, et al., Spatiotemporal dynamics of word processing in the human brain, Frontiers in Neuroscience 1 (1) (2007) 185–196.
[28] N. Swann, N. Tandon, R. Canolty, T.M. Ellmore, L.K. McEvoy, S. Dreyer, et al., Intracranial EEG reveals a time- and frequency-specific role for the right inferior frontal gyrus and primary motor cortex in stopping initiated responses, Journal of Neuroscience 29 (40) (2009) 12675–12685.
[29] C. Studholme, E. Novotny, I.G. Zubal, J.S. Duncan, Estimating tissue deformation between functional images induced by intracranial electrode implantation using anatomical MRI, NeuroImage 13 (4) (2001) 561–576.
[30] D. Hermes, K.J. Miller, H.J. Noordmans, M.J. Vansteensel, N.F. Ramsey, Automated electrocorticographic electrode localization on individually rendered brain surfaces, Journal of Neuroscience Methods 185 (2) (2010) 293–298.
[31] S.S. Dalal, E. Edwards, H.E. Kirsch, N.M. Barbaro, R.T. Knight, S.S. Nagarajan, Localization of neurosurgically implanted electrodes via photograph-MRI-radiograph coregistration, Journal of Neuroscience Methods 174 (1) (2008) 106–115.
[32] U. Mitzdorf, Properties of the evoked potential generators: current source-density analysis of visually evoked potentials in the cat cortex, The International Journal of Neuroscience 33 (1–2) (1987) 33–59.
[33] A. Destexhe, D. Contreras, M. Steriade, Spatiotemporal analysis of local field potentials and unit discharges in cat cerebral cortex during natural wake and sleep states, Journal of Neuroscience 19 (11) (1999) 4595–4608.
[34] J.M. Palva, S. Monto, S. Kulashekhar, S. Palva, Neuronal synchrony reveals working memory networks and predicts individual memory capacity, Proceedings of the National Academy of Sciences of the United States of America 107 (16) (2010) 7580–7585.
[35] C. Tallon-Baudry, The roles of gamma-band oscillatory synchrony in human visual cognition, Frontiers in Bioscience 14 (2009) 321–332.
[36] C. Tallon-Baudry, O. Bertrand, F. Peronnet, J. Pernier, Induced gamma-band activity during the delay of a visual short-term memory task in humans, Journal of Neuroscience 18 (11) (1998) 4244–4254.
[37] Q. Luo, D. Mitchell, X. Cheng, K. Mondillo, D. McCaffrey, T. Holroyd, et al., Visual awareness, emotion, and gamma band synchronization, Cerebral Cortex 19 (8) (2009) 1896–1904.
[38] R. Levy, P.S. Goldman-Rakic, Segregation of working memory functions within the dorsolateral prefrontal cortex, Experimental Brain Research Experimentelle Hirnforschung 133 (1) (2000) 23–32.
[39] M. Urbanski, M. Thiebaut de Schotten, S. Rodrigo, M. Catani, C. Oppenheim, E. Touze, et al., Brain networks of spatial awareness: evidence from diffusion tensor imaging tractography, Journal of Neurology, Neurosurgery, and Psychiatry 79 (5) (2008) 598–601.
[40] M.F. Kraus, T. Susmaras, B.P. Caughlin, C.J. Walker, J.A. Sweeney, D.M. Little, White matter integrity and cognition in chronic traumatic brain injury: a diffusion tensor imaging study, Brain 130 (Pt 10) (2007) 2508–2519.
[41] E. Rykhlevskaia, L.Q. Uddin, L. Kondos, V. Menon, Neuroanatomical correlates of developmental dyscalculia: combined evidence from morphometry and tractography, Frontiers in Human Neuroscience 3 (2009) 51.
[42] H.S. Kudrimoti, C.A. Barnes, B.L. McNaughton, Reactivation of hippocampal cell assemblies: effects of behavioral state, experience, and EEG dynamics, Journal of Neuroscience 19 (10) (1999) 4090–4101.
[43] A.K. Liu, J.W. Belliveau, A.M. Dale, Spatiotemporal imaging of human brain activity using functional MRI constrained magnetoencephalography data: Monte Carlo simulations, Proceedings of the National Academy of Sciences of the United States of America 95 (15) (1998) 8945–8950.
[44] R.T. Canolty, E. Edwards, S.S. Dalal, M. Soltani, S.S. Nagarajan, H.E. Kirsch, et al., High gamma power is phase-locked to theta oscillations in human neocortex, Science (New York, NY) 313 (5793) (2006) 1626–1628.
[45] S.D. Slotnick, L.R. Moo, M.A. Kraut, R.P. Lesser, J. Hart Jr., Interactions between thalamic and cortical rhythms during semantic memory recall in human, Proceedings of the National Academy of Sciences of the United States of America 99 (9) (2002) 6440–6443.
[46] L.J. Bour, M.F. Contarino, E.M. Foncke, R.M. de Bie, P. van den Munckhof, J.D. Speelman, et al., Long-term experience with intraoperative microrecording during DBS neurosurgery in STN and GPI (2010)Acta Neurochirurgica (2010).
[47] D.A. Gutman, P.E. Holtzheimer, T.E. Behrens, H. Johansen-Berg, H.S. Mayberg, A tractography analysis of two deep brain stimulation white matter targets for depression, Biological Psychiatry 65 (4) (2009) 276–282.
[48] N.K. Logothetis, The neural basis of the blood-oxygen-level-dependent functional magnetic resonance imaging signal, Philosophical Transactions of the Royal Society of London 357 (1424) (2002) 1003–1037.
[49] A. Ekstrom, N. Suthana, D. Millett, I. Fried, S. Bookheimer, Correlation between BOLD fMRI and theta-band local field potentials in the human hippocampal area, Journal of Neurophysiology 101 (5) (2009) 2668–2678.
[50] D.K. Murphey, D. Yoshor, M.S. Beauchamp, Perception matches selectivity in the human anterior color center, Current Biology 18 (3) (2008) 216–220.
[51] R. Matsumoto, D.R. Nair, E. LaPresto, I. Najm, W. Bingaman, H. Shibasaki, et al., Functional connectivity in the human language system: a cortico-cortical evoked potential study, Brain 127 (Pt 10) (2004) 2316–2330.
[52] T.M. Ellmore, M.S. Beauchamp, T.J. O'Neill, S. Dreyer, N. Tandon, Relationships between essential cortical language sites and subcortical pathways, Journal of Neurosurgery 111 (4) (2009) 755–766.

Please cite this article as: K. Tertel, et al., Probing brain connectivity by combined analysis of diffusion MRI tractography and electrocorticography, Comput. Biol. Med. (2010), doi:10.1016/j.compbiomed.2010.11.004